

LETTER TO THE EDITOR

Neutral chlorine and molecular hydrogen at high redshift

S.A. Balashev^{1,2}, P. Noterdaeme³, V.V. Klimenko^{1,2}, P. Petitjean³,
R. Srianand⁵, C. Ledoux⁴, A.V. Ivanchik^{1,2}, and D.A. Varshalovich^{1,2}

¹ Ioffe Physical-Technical Institute of RAS, Polytekhnicheskaya 26, 194021 Saint-Petersburg, Russia

² St.-Petersburg Polytechnic University, Polytekhnicheskaya 29, 195251 Saint-Petersburg, Russia

³ Institut d'Astrophysique de Paris, CNRS-UPMC, UMR7095, 98bis bd Arago, 75014 Paris, France

⁴ European Southern Observatory, Alonso de Córdova 3107, Vitacura, Casilla 19001, Santiago 19, Chile

⁵ Inter-University Centre for Astronomy and Astrophysics, Post Bag 4, Ganeshkhind, 411 007 Pune, India

Accepted 28/01/2015, Received 19/12/2014

ABSTRACT

Chlorine and molecular hydrogen are known to be tightly linked together in the cold phase of the local interstellar medium through rapid chemical reactions. We present here the first systematic study of this relation at high redshifts using H₂-bearing damped Ly α systems (DLAs) detected along quasar lines of sight. Using high-resolution spectroscopic data from VLT/UVES and Keck/HIRES, we report the detection of Cl I in 9 DLAs (including 5 new detections) out of 18 high- z DLAs with $N(\text{H}_2) \geq 10^{17.3} \text{ cm}^{-2}$ (including a new H₂ detection at $z = 3.09145$ towards J2100–0641) and present upper limits for the remaining 9 systems. We find a $\sim 5\sigma$ correlation between $N(\text{Cl I})$ and $N(\text{H}_2)$ with only ~ 0.2 dex dispersion over the range $18.1 < \log N(\text{H}_2) < 20.1$, thus probing column densities 10 times lower those seen towards nearby stars, roughly following the relation $N(\text{Cl I}) \approx 1.5 \times 10^{-6} \times N(\text{H}_2)$. This relation between column densities is surprisingly the same at low and high redshift suggesting that the physical and chemical conditions are similar for a given H₂ (or Cl I) column density. In turn, the $N(\text{Cl I})/N(\text{H}_2)$ ratio is found to be uncorrelated with the overall metallicity in the DLA. Our results confirm that neutral chlorine is an excellent tracer of molecule-rich gas and show that the molecular fraction or/and metallicity in the H₂-bearing component of DLA could possibly be much higher than the line-of-sight average values usually measured in DLAs.

Key words. cosmology: observations – ISM: clouds – quasar: absorption lines

1. Introduction

It has been shown that the global star-formation rate in the Universe gradually increases from $z \sim 10$ to $z \sim 2-3$ and then steeply decreases till the present epoch, $z = 0$ (see e.g. Dunlop 2011, and references therein). Because metals are produced by stars, the determination of metal abundance in the gas provides complementary information about star-formation history (Rafelski et al. 2012). This can be done using Damped Lyman- α absorption systems (DLAs) that represent the main reservoir of neutral gas at high redshift (Prochaska & Wolfe 2009; Noterdaeme et al. 2009) and are likely to be located in galaxies or in their close environment (e.g. Krogager et al. 2012). DLAs arise mostly in the warm neutral medium (e.g. Petitjean et al. 2000; Kanekar et al. 2014) and have a multicomponent velocity structure, with metal absorption lines spread typically over 100–500 km s^{−1} (Ledoux et al. 1998). In a small fraction of DLAs, the line of sight intercepts cold gas, as traced by molecular hydrogen (e.g. Noterdaeme et al. 2008, 2011; Balashev et al. 2014) and/or 21-cm absorption (e.g. Srianand et al. 2012). Important progress has been made towards understanding the properties of the gas (through e.g. deriving physical conditions Srianand et al. 2005; Noterdaeme et al. 2007a; Jorgenson et al. 2009 and physical extent Balashev et al. 2011) and the incidence of cold gas in DLAs has been related to other properties (such as the metallicity (Petitjean et al. 2006) or the dust content (Ledoux et al. 2003; Noterdaeme et al. 2008)). However, due to the strong saturation of H I Lyman series lines, it remains impossible to directly deter-

mine the H I column density associated with the individual cold gas components traced by H₂ absorption. Even for metals, whose absorption lines are not saturated, it is very difficult to determine what fraction originates from the cold phase. Difficulties arise as well with the 21-cm absorption that do not always exactly coincide with H₂ absorption (Srianand et al. 2013) although it could be due to the different structures of the optical and radio emitting regions of the background quasars. Out of all the metals, chlorine shows a unique behavior in the presence of H₂. Because the ionization potential of chlorine (12.97 eV) is less than that of atomic hydrogen, chlorine is easily ionized in the diffuse neutral medium. However, this species reacts exothermically with H₂ at a very high rate converting rapidly Cl⁺ into HCl⁺. The latter subsequently releases neutral chlorine through several channels (Jura 1974; Neufeld & Wolfire 2009). This process is so efficient that chlorine is completely neutral in presence of a small amount of H₂. In our Galaxy the fact that chlorine abundance anti-correlates with the average number density along the line of sight (Harris & Bromage 1984; Jenkins et al. 1986) has been interpreted as chlorine depletion. However, models predict as well as observations indicate, that gas with moderate dust content presents negligible depletion of chlorine (e.g. Neufeld & Wolfire 2009; Savage & Sembach 1996; Jenkins 2009). Observationally, a tight relation is indeed found between Cl I and H₂ in the local ISM (Jura 1974; Sonnentrucker et al. 2006; Moomey et al. 2012). In this letter, we present the first study of this relation at high redshift and over a wide range of column densities.

2. Data sample and measurements

Since the first detection by Levshakov & Varshalovich (1985), about two dozen H_2 absorption systems have been detected at high redshifts in QSO spectra. The detection limit of the strongest Cl I absorption line (1347\AA , $f=0.0153$ (Schechtman et al. 1993)) in high quality spectrum ($S/N \sim 50$, $R \sim 50\,000$) corresponds to $N(\text{Cl I}) \sim 10^{12} \text{ cm}^{-2}$. The solar abundance of chlorine is $10^{-6.5}$ that of hydrogen (Asplund et al. 2009) and given previous measurements of $N(\text{Cl I})/2N(\text{H}_2)$ (e.g. Moomey et al. 2012) we conservatively limit our study to systems with $N(\text{H}_2) \gtrsim 10^{17} \text{ cm}^{-2}$.

Redshifts, H I and H_2 column densities, and metallicities were mainly taken from the literature and are based on VLT/UVES, Keck/HIRES or HST/STIS data. We refitted H_2 absorption systems towards Q 2123–0050 and Q J2340–0053 to take into account the positions of the detected Cl I components. We also detect a new H_2 absorption system in the $z = 3.09$ DLA towards J 2100–0641 in which Jorgenson et al. (2010) have reported the presence of neutral carbon. C I is indeed known to be an excellent indicator of the presence of molecules (e.g. Srianand et al. 2005). We used the MAKEE package (T. Burles) to reduce archival data from this quasar obtained in 2005, 2006 and 2007 under programs U17H (PI: Prochaska), G400H (PI: Ellison) and U149Hr (PI: Wolfe). We have found strong H_2 absorption lines from rotational levels up to $J = 5$ (see Fig. 1) at $z = 3.091485$ with a total column density of $\log N(\text{H}_2) = 18.76 \pm 0.03$.

For all systems we retrieved data from the VLT/UVES or the Keck/HIRES archives. We reduced the data and fitted the lines using profile fitting. Neutral chlorine is detected in nine DLAs (Fig 2). Four detections were already reported in the literature: Q 1232+082 (Balashev et al. 2011), Q 0812–3208 (Prochaska et al. 2003), Q 1237+0647 (Noterdaeme et al. 2010) and Q 2140–0321 (Noterdaeme et al. submitted). The remaining five are new detections. We measured upper-limits of $N(\text{Cl I})$ for the remaining nine systems. We used mainly the 1347\AA Cl I line. Whenever possible, we also used Cl I lines at 1088\AA , 1188\AA , 1084\AA , 1094\AA and 1085\AA , with oscillator strength from respectively Schechtman et al. (1993), Morton (2003), Morton (2003), Sonnentrucker et al. (2006) and Oliveira & Hébrard (2006).

Table 1 summarizes the results of Cl I measurements. We have kept all components with $\log N(\text{H}_2) > 17$. We did not use two known H_2 absorption systems towards Q 0013–0029 and J 091826.16+163609.0 since H_2 column densities in these systems are not well defined.

3. Results

Fig. 3 shows the Cl I column density, $N(\text{Cl I})$, versus $N(\text{H}_2)$ and compares our high- z measurements to those obtained in the local ISM using the Copernicus satellite (Moomey et al. 2012). As can be seen our high- z measurements extend the relation to H_2 column densities ten times smaller than those measured in the local ISM. Cl I and H_2 are found to be very well correlated ($r = 0.95$) over the entire $N(\text{H}_2)$ range. It is striking that measurements at high and low redshifts are indistinguishable in the overlapping regime ($\log N(\text{H}_2) \sim 19\text{--}20.2$). The correlation is seen over about three orders of magnitude in column density with a dispersion of about 0.2 dex only. A least-squares bisector linear fit provides a slope of 0.83 and 0.87 for the high- z and $z = 0$ data, respectively, with an almost equal normalization ($\log N(\text{Cl I}) \approx 13.7$ at $\log N(\text{H}_2) = 20$). We note that the upper limits on $N(\text{Cl I})$ lie mostly at the low $N(\text{H}_2)$ end and are least constraining since they

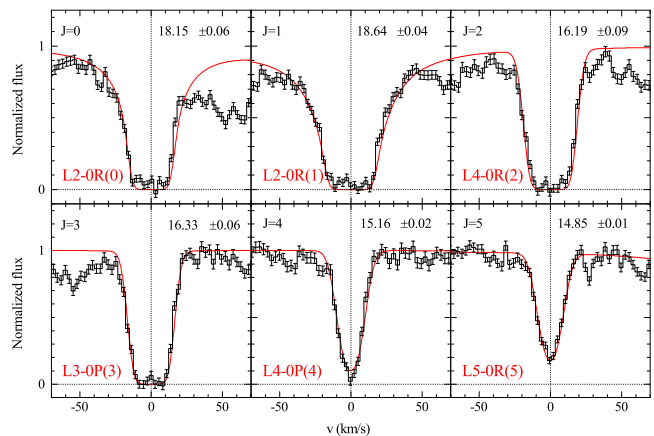


Fig. 1. Voigt profile fits to the newly detected H_2 absorption lines from rotational levels $J=0$ to $J=5$ at $z = 3.091485$ towards J 2100–0641. The column densities are indicated (in $\log(\text{cm}^{-2})$) in the top right corner of each panel.

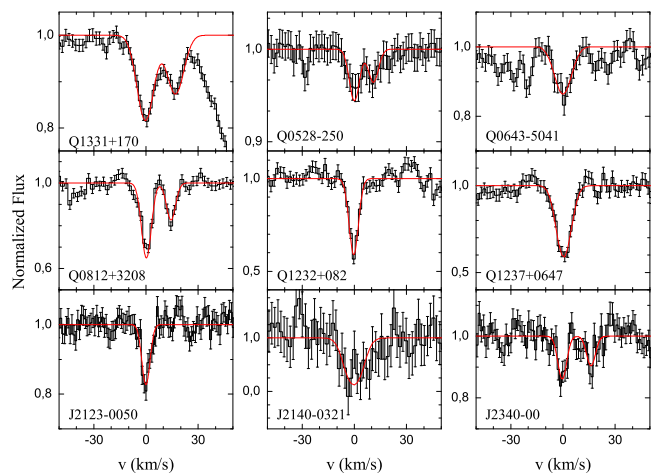


Fig. 2. Voigt profile fits to $\text{Cl I } \lambda 1347$ absorption lines associated with high- z strong H_2 absorption systems.

are compatible with the values expected from the above relation. For this reason, we will not consider them further in the discussion but still include them in the figures for completeness. The slopes are less than one, meaning that the $\text{Cl I}/\text{H}_2$ ratio slightly decreases with increasing $N(\text{H}_2)$. This is unlikely to be due to conversion of Cl into H_2Cl^+ and/or HCl , since chlorine chemistry models (Neufeld & Wolfire 2009) as well as measurements (e.g. towards Sgr B2(S), Lis et al. 2010) show that in diffuse molecular clouds only $\sim 1\%$ of chlorine is in the molecular form. A < 1 slope could in principle be due to dust depletion. However, there is no trend for increasing Cl depletion with increasing H_2 or Cl I column densities in Galactic clouds (see Moomey et al. 2012). In addition, for high redshift measurements, elemental abundance pattern (Noterdaeme et al. 2008) as well as direct measurements (e.g. Noterdaeme et al. 2010) indicate $A_V < 0.2$ when modeling of chlorine chemistry (Neufeld & Wolfire 2009) shows that for such low extinction ($A_V < 1$) all chlorine is in the gas phase.

A possibility is thus that the molecular fraction in the gas probed by Cl I is slightly increasing with increasing $N(\text{H}_2)$. It can be expected since H_2 self-shielding increase while Cl I is already completely in the neutral form. Finally, the similarity between

Table 1. Measurements of Cl I in strong H₂ absorption systems at high redshift.

Quasar	<i>z</i> _{em}	<i>z</i> _{DLA}	log <i>N</i> (H I)	[X/H]	X	Ref.	<i>z</i> _{H2}	log <i>N</i> (H ₂)	log <i>N</i> (Cl I)	<i>b</i> (km s ⁻¹)	[Cl I/H ₂]
Q 0027–1836	2.56	2.40	21.75±0.10	-1.63±0.10	Zn	1	2.40183	17.30±0.07	< 12.71	—	< 1.61
Q 0405–4418	3.02	2.59	21.75±0.10	-1.12±0.10	Zn	2	2.59475	18.14±0.07	< 12.71	—	< 0.77
Q 0528–2505	2.77	2.81	21.35±0.07	-0.91±0.07	Zn	3	2.81098	18.11±0.02	11.92±0.08	4.1±1.5	0.01±0.08
							2.81112	17.85±0.02	11.73±0.11	4.2±2.0	0.08±0.11
Q 0551–3637	2.32	1.96	20.70±0.08	-0.35±0.08	Zn	4	1.96214	17.42 ^{+0.45} _{-0.73}	< 12.40	—	< 1.54
Q J0643–5041	3.09	2.66	21.03±0.08	-0.91±0.09	Zn	5	2.65860	18.54±0.01	12.51±0.05	5.8±1.4	0.17±0.05
Q J0812+3208	2.7	2.63	21.35±0.10	-0.81±0.10	Zn	6	2.62628	18.84±0.06	12.79±0.05	2.0±0.6	0.15±0.08
							2.62644	19.93±0.01	13.78±0.27	0.17±0.05	0.05±0.27
Q J0816+1446	3.84	3.29	22.00±0.10	-1.10±0.10	Zn	7	3.2874	18.62±0.18	< 13.65	—	< 1.23
							3.28667	17.60±0.27	< 12.76	—	< 1.36
Q 1232+0815	2.57	2.34	20.90±0.08	-1.35±0.12	S	8	2.33772	19.57±0.10	13.49±0.08	0.8±0.2	0.12±0.13
Q J1237+0647	2.78	2.69	20.00±0.15	+0.34±0.12	Zn	9	2.68959	19.20±0.13	13.01±0.02	4.5±0.4	0.01±0.13
Q 1331+170	2.08	1.78	21.18±0.04	-1.22±0.10	Zn	10,11	1.77636	19.71±0.10	12.87±0.02	5.7±0.5	-0.64±0.10
Q J1439+1118	2.58	2.42	20.10±0.10	+0.16±0.11	Zn	12	2.4184	19.38±0.04	< 13.25	—	< 0.07
Q 1441+2737	4.42	4.22	20.95±0.08	-0.63±0.10	S	13	4.22401	18.05±0.05	< 12.86	—	< 1.01
							4.22371	17.91±0.03	< 12.66	—	< 0.95
Q 1444+0126	2.21	2.09	20.25±0.07	-0.80±0.09	Zn	14	2.08696	18.16±0.11	< 12.42	—	< 0.46
Q J2100–0641	3.14	3.09	21.05±0.15	-0.73±0.15	Si	15	3.09149	18.76±0.03	< 12.86	—	< 0.3
Q J2123–0050	2.26	2.06	19.18±0.15	-0.19±0.10	S	16	2.05933	18.09±0.02	12.27±0.06	2.6±0.5	0.38±0.06
Q J2140–0321	2.48	2.34	22.40±0.10	-1.05±0.13	P	17	2.33995	20.13±0.07	13.67±0.15	5–10	-0.26±0.18
Q J2340–0053	2.09	2.05	20.35±0.15	-0.92±0.03	Zn	15	2.05456	18.07±0.06	12.25±0.15	0.8±0.6	0.38±0.16
							2.05473	18.25±0.05	12.13±0.18	1.0±1.0	0.08±0.19
Q 2348–0108	3.01	2.43	20.50±0.10	-0.62±0.10	S	18,19	2.42688	18.12±0.37	< 13.86	—	< 1.94
							2.42449	17.52±0.80	< 13.13	—	< 0.81

References. (1) Noterdaeme et al. (2007a); (2) Ledoux et al. (2003); (3) Noterdaeme et al. (2008); (4) Ledoux et al. (2002); (5) Alborno Vázquez et al. (2014); (6) Jorgenson et al. (2009); (7) Guimarães et al. (2012); (8) Balashev et al. (2011); (9) Noterdaeme et al. (2010); (10) Carswell et al. (2011); (11) Balashev et al. (2010); (12) Srianand et al. (2008); (13) Ledoux et al. (2006); (14) Ledoux et al. (2003); (15) Jorgenson et al. (2010); (16) Malec et al. (2010); (17) Noterdaeme et al. submitted; (18) Petitjean et al. (2006); (19) Noterdaeme et al. (2007b).

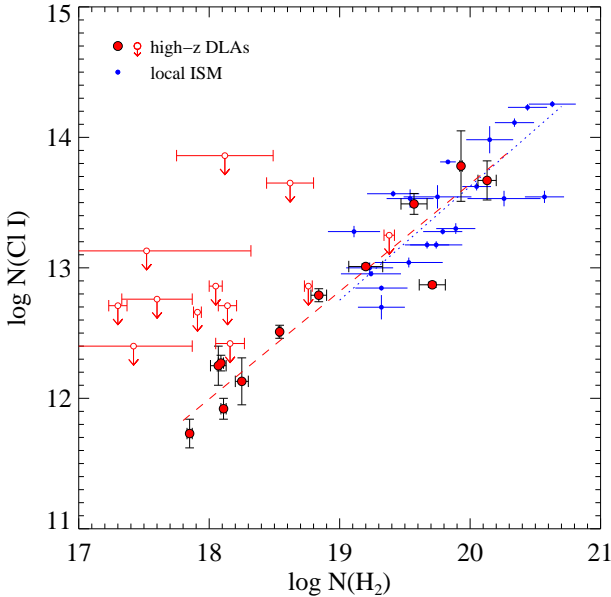


Fig. 3. Column densities of Cl I versus that of H₂. The red and blue points indicate the measurements at high redshift (this work) and in our Galaxy (Mooney et al. 2012), respectively. The straight (dashed, dotted) lines show the respective least-squares bisector fits to the data.

our Galaxy and high-*z* measurements at $\log N(\text{H}_2) \geq 19$ might indicate that the chemical and physical conditions in the cold gas can be similar, otherwise fine tuning would be required between

the different factors that impact on the $N(\text{Cl I})$ to $N(\text{H}_2)$ ratio (e.g. number density, metallicity, dust content and UV flux).

Before continuing further, we note that in H₂-bearing gas, chlorine is found exclusively in the neutral form (i.e. $N(\text{Cl}) = N(\text{Cl I})$) (e.g. Jura 1974). Since we expect that all chlorine is in gas-phase¹, the abundance of chlorine, $[\text{Cl}/\text{H}]$, in H₂-bearing gas can be expressed as

$$[\text{Cl}/\text{H}] = [\text{Cl I}/\text{H}_2] + \log f, \quad (1)$$

where

$$[\text{Cl I}/\text{H}_2] = \log \left(\frac{N(\text{Cl I})}{2N(\text{H}_2)} \right) - \log \left(\frac{\text{Cl}}{\text{H}} \right)_{\odot} \quad (2)$$

and $f = 2N(\text{H}_2)/(2N(\text{H}_2) + N(\text{H I}))$ is the molecular fraction. Therefore the ratio $[\text{Cl I}/\text{H}_2]$ gives a direct constraint on the chlorine-based metallicity of H₂-bearing gas provided the molecular fraction of H₂-bearing gas is known. Conversely, if a constraint can be put on the actual chlorine abundance, $[\text{Cl I}/\text{H}_2]$ can provide an estimate of the amount of H I present in H₂-bearing gas. If Cl is depleted onto dust grains then the mentioned estimates of metallicity and molecular fraction will have to be corrected from the Cl depletion factor.

The Fig. 4 shows $[\text{Cl I}/\text{H}_2]$ as a function of the overall metallicity for DLAs (given in Table 1) at high redshift or as a function of $[\text{Cl}/\text{H}]$ for clouds in our Galaxy. Since $f \leq 1$, $[\text{Cl I}/\text{H}_2]$ gives an upper limit on the metallicity in H₂-bearing gas, which is found to be roughly equal or less than solar metallicity. For

¹ We note that the presence of Cl II in the outer envelope of the H₂ cloud is not excluded, but it does not influence our derivation

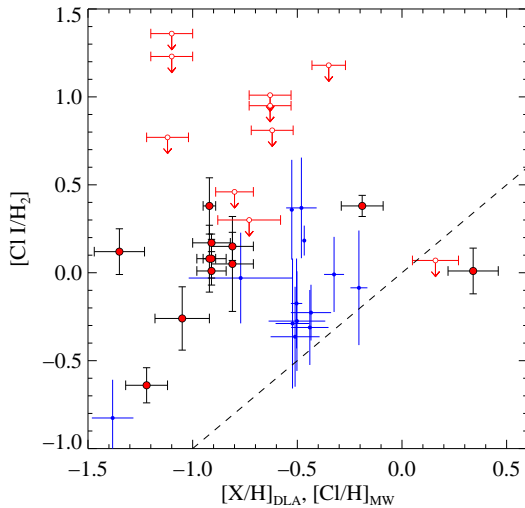


Fig. 4. $[\text{Cl I}/\text{H}_2]$ as a function of the *overall* metallicity for high- z DLAs (red points) and the chlorine-based metallicity for Milky-Way clouds (blue points). The dashed line represents the one-to-one relation.

13 out of 21 Cl I bearing clouds in our Galaxy associated Cl II was measured (Moomey et al. 2012). Therefore we have estimated the overall chlorine abundance $[\text{Cl}/\text{H}]$ of these clouds as $(N(\text{Cl I}) + N(\text{Cl II})) / (N(\text{H I}) + 2N(\text{H}_2))$ (shown by blue circles in Fig. 4). Unfortunately, for high redshift DLAs, not only Cl II is not detected but also DLAs contain several H I clouds so that chlorine abundance of the very cloud of interest cannot be measured. Therefore we consider the overall metallicity (averaged over velocity components) measured using another non-depleted element (usually Zn or S, see Table 1). In Fig. 4 it can be seen that the $[\text{Cl I}/\text{H}_2]$ ratio is likely not correlated with the *overall* metallicity of the DLA (Pearson correlation coefficient 0.3 at 0.3 significance level). For Milky-Way clouds it can be seen that $[\text{Cl}/\text{H}]$ is typically one third solar, which can be interpreted as evidence for chlorine depletion (Moomey et al. 2012).

The large difference between $[\text{Cl I}/\text{H}_2]$ and $[\text{X}/\text{H}]_{\text{DLA}}$ for the high redshift clouds can be explained either by a molecular fraction $f < 1$ in H_2 -bearing clouds or by a higher metallicity in the H_2 -bearing gas compared to the overall DLA metallicity or by both effects. If we assume that the metallicity in the H_2 -bearing gas is equal to the overall DLA metallicity we find (using Eq. 1) that the molecular fraction in the H_2 -bearing gas is typically an order of magnitude higher than the overall inferred DLA molecular fraction. Interestingly, two systems sitting close to the one-to-one relation are those where CO molecules have been detected (Q 1439+1118 and Q 1237+0647). In such systems, the H_2 component is probably fully molecularized and its metallicity is close to the overall metallicity of the DLA.

4. Conclusion

We have studied the neutral chlorine abundance in high redshift ($z \sim 2-4$) strong H_2 bearing DLAs with $\log N(\text{H}_2) > 17.3$. These systems arise in the cold neutral medium of galaxies in the early Universe. We have used 17 systems from the literature and also present a new H_2 detection at $z = 3.09145$ in the spectrum of J 2100–0641. We have detected Cl I absorption lines in half of these systems, including 5 new detections. The derived upper limits for $N(\text{Cl I})$ for the remaining systems are shown to be consistent with the behavior of the overall population. Our measurements extend the Cl I- H_2 relation to lower column densities than measurements towards nearby stars. We show that there is

a 5σ correlation between the column densities of both species over the range $18.1 < \log N(\text{H}_2) < 20.1$ with indistinguishable behavior between high and zero redshift systems. This suggests that at a given $N(\text{H}_2)$ the physical conditions are likely similar in our Galaxy and high- z gas, in spite of possible differences in the dust depletion levels. As we expect the Cl to be depleted less in the high- z absorbers studied here, we use the abundance of chlorine with respect to H_2 to constrain the molecular fraction and the metallicity in H_2 -bearing gas. Our results suggest that the molecular fraction and/or the metallicity in the H_2 and Cl I bearing components could be much higher than the mean value measured over the whole DLA system. This implies that a large fraction of H I is unrelated to the cold phase traced by H_2 . Finally, our understanding of the formation of H_2 onto dust grains, self-shielding and lifetime of cold diffuse gas would certainly benefit from further observations of chlorine and molecular hydrogen in different environments and over a wide range of column densities.

Acknowledgments. SB and VK thank RF President Program (grant MK-4861.2013.2) and “Leading Scientific Schools of Russian Federation” (grant NSh-294.2014.2). RS and PPJ gratefully acknowledge support from the Indo-French Centre for the Promotion of Advanced Research (Centre Franco-Indien pour la Promotion de la Recherche Avancée) under contract No. 4304-2.

References

- Albornoz Vázquez, D., Rahmani, H., Noterdaeme, P., et al. 2014, A&A, 562, A88
- Asplund, M., Grevesse, N., Sauval, A. J., & Scott, P. 2009, ARA&A, 47, 481
- Balashev, S. A., Ivanchik, A. V., & Varshalovich, D. A. 2010, Astronomy Letters, 36, 761
- Balashev, S. A., Klimenko, V. V., Ivanchik, A. V., et al. 2014, MNRAS, 440, 225
- Balashev, S. A., Petitjean, P., Ivanchik, A. V., et al. 2011, MNRAS, 418, 357
- Carswell, R. F., Jorgenson, R. A., Wolfe, A. M., & Murphy, M. T. 2011, MNRAS, 411, 2319
- Dunlop, J. S. 2011, Science, 333, 178
- Guimarães, R., Noterdaeme, P., Petitjean, P., et al. 2012, AJ, 143, 147
- Harris, A. W. & Bromage, G. E. 1984, MNRAS, 208, 941
- Jenkins, E. B. 2009, ApJ, 700, 1299
- Jenkins, E. B., Savage, B. D., & Spitzer, Jr., L. 1986, ApJ, 301, 355
- Jorgenson, R. A., Wolfe, A. M., & Prochaska, J. X. 2010, ApJ, 722, 460
- Jorgenson, R. A., Wolfe, A. M., Prochaska, J. X., & Carswell, R. F. 2009, ApJ, 704, 247
- Jura, M. 1974, ApJ, 190, L33
- Kanekar, N., Prochaska, J. X., Smette, A., et al. 2014, MNRAS, 438, 2131
- Krogager, J.-K., Fynbo, J. P. U., Möller, P., et al. 2012, MNRAS, 424, L1
- Ledoux, C., Petitjean, P., Bergeron, J., Wampler, E. J., & Srianand, R. 1998, A&A, 337, 51
- Ledoux, C., Petitjean, P., & Srianand, R. 2003, MNRAS, 346, 209
- Ledoux, C., Petitjean, P., & Srianand, R. 2006, ApJ, 640, L25
- Ledoux, C., Srianand, R., & Petitjean, P. 2002, A&A, 392, 781
- Levshakov, S. A. & Varshalovich, D. A. 1985, MNRAS, 212, 517
- Lis, D. C., Pearson, J. C., Neufeld, D. A., et al. 2010, A&A, 521, L9
- Malec, A. L., Buning, R., Murphy, M. T., et al. 2010, MNRAS, 403, 1541
- Moomey, D., Federman, S. R., & Sheffer, Y. 2012, ApJ, 744, 174
- Morton, D. C. 2003, ApJS, 149, 205
- Neufeld, D. A. & Wolfire, M. G. 2009, ApJ, 706, 1594
- Noterdaeme, P., Ledoux, C., Petitjean, P., et al. 2007a, A&A, 474, 393
- Noterdaeme, P., Ledoux, C., Petitjean, P., & Srianand, R. 2008, A&A, 481, 327
- Noterdaeme, P., Petitjean, P., Ledoux, C., et al. 2010, A&A, 523, A80
- Noterdaeme, P., Petitjean, P., Ledoux, C., & Srianand, R. 2009, A&A, 505, 1087
- Noterdaeme, P., Petitjean, P., Srianand, R., Ledoux, C., & Le Petit, F. 2007b, A&A, 469, 425
- Noterdaeme, P., Petitjean, P., Srianand, R., Ledoux, C., & López, S. 2011, A&A, 526, L7
- Oliveira, C. M. & Hébrard, G. 2006, ApJ, 653, 345
- Petitjean, P., Ledoux, C., Noterdaeme, P., & Srianand, R. 2006, A&A, 456, L9
- Petitjean, P., Srianand, R., & Ledoux, C. 2000, A&A, 364, L26
- Prochaska, J. X., Howk, J. C., & Wolfe, A. M. 2003, Nature, 423, 57
- Prochaska, J. X. & Wolfe, A. M. 2009, ApJ, 696, 1543
- Rafelski, M., Wolfe, A. M., Prochaska, J. X., Neeleman, M., & Mendez, A. J. 2012, ApJ, 755, 89

- Savage, B. D. & Sembach, K. R. 1996, *ARA&A*, 34, 279
- Schechtman, R. M., Federman, S. R., Beideck, D. J., & Ellis, D. J. 1993, *ApJ*, 406, 735
- Sonnentrucker, P., Friedman, S. D., & York, D. G. 2006, *ApJ*, 650, L115
- Srianand, R., Gupta, N., Petitjean, P., et al. 2012, *MNRAS*, 421, 651
- Srianand, R., Gupta, N., Rahmani, H., et al. 2013, *MNRAS*, 428, 2198
- Srianand, R., Noterdaeme, P., Ledoux, C., & Petitjean, P. 2008, *A&A*, 482, L39
- Srianand, R., Petitjean, P., Ledoux, C., Ferland, G., & Shaw, G. 2005, *MNRAS*, 362, 549